IIETA International Information and Engineering Technology Association
Advancing the World of Information and Engineering

Annales de Chimie - Science des Matériaux
Vol. 50, No. 5, October, 2026, pp. 445-450
Journal homepage: http://iieta.org/journals/acsm

Structure and Wear Resistance of Carburized Iron–Chromium Coatings for Restoring Precision Diesel Fuel Components

Vladimir A. Konchin*, Vladimir I. Serebrovsky, Aleksandr A. Merkulov, Vladislav S. Fetisov

Kursk State Agrarian University named after I.I. Ivanov, Kursk 305021, Russia

Corresponding Author Email: konchin98@mail.ru

Copyright: ©2026 The authors. This article is published by IIETA and is licensed under the CC BY 4.0 license (http://creativecommons.org/licenses/by/4.0/).

https://doi.org/10.18280/acsm.500503

Received: 13 June 2026
Revised: 9 August 2026
Accepted: 24 August 2026
Available online: 31 October 2026

Keywords:
carburizing, coating structure, iron–chromium coating, plunger pair, restoration, wear resistance

ABSTRACT

Wear of precision components in diesel fuel equipment limits the service life of fuel pumps and makes effective restoration technologies necessary. This study evaluates how carburizing and subsequent heat treatment affect the structure, chromium content, hardness, seizure resistance, and wear resistance of electrodeposited iron-chromium coatings for plunger-pair restoration. Coatings were deposited on KhVG steel from a sulfate electrolyte containing chromium nitrate under asymmetric alternating current, carburized in an active carbon-based paste at 860–950 °C, oil-quenched, and tempered. Optical and scanning electron microscopy (SEM), energy-dispersive X-ray spectroscopy (EDS), Rockwell C hardness (HRC) measurements, and disk–block tribological tests were used. The as-deposited coatings exhibited a pronounced layered structure. Carburizing reduced structural heterogeneity and produced a carbide-enriched diffusion layer. The most favorable combination of diffusion-layer development and hardness was obtained at approximately 1.5–2.0 wt.% Cr. Quenching from 840–860 °C produced the highest hardness. Carburizing at 920–940 °C increased seizure resistance and reduced mass loss in diesel fuel by approximately three times compared with coatings carburized at 860 °C. The results support the use of carburized iron–chromium coatings as a restoration route for precision plunger pairs; long-term bench and field endurance tests are still required before equivalence with new components can be claimed.

1. INTRODUCTION

The operating stability of diesel fuel-injection equipment depends strongly on the condition of precision mating surfaces in high-pressure pumps and injectors. Particulate contamination and progressive wear alter the clearances of precision pairs, disturb fuel delivery, and may ultimately lead to loss of functional performance [1, 2]. Tribological studies of candidate plunger materials further show that scuffing resistance in diesel-like fuels is controlled by both surface condition and material/coating selection [3].

Surface restoration is therefore attractive when dimensional accuracy can be recovered without sacrificing hardness and seizure resistance. Conventional hard chromium has long been used because of its high hardness and wear resistance, but Cr(VI)-based processes raise environmental and occupational concerns, and hard-chromium deposits may contain crack networks and residual stresses. These limitations have intensified interest in Cr(III)-based electrodeposition and in alternative wear-resistant electrodeposited alloys [4-8].

Recent Cr(III) electrodeposition studies demonstrate that bath composition, temperature, current regime, and alloying additions can markedly change deposit morphology and mechanical behavior [4-6]. Electrodeposited Fe–Cr films are also of interest because chromium incorporation can modify structure and hardness while retaining an iron-rich matrix that is technologically compatible with ferrous substrates [9]. This combination is relevant to repair coatings, where both deposit build-up rate and response to subsequent heat treatment are important.

For iron-based surface layers, carburizing provides an additional route for increasing near-surface carbon content and forming hard carbide-rich structures. Studies on carburized iron and carburized steels show that carbon enrichment and subsequent heat treatment can increase hardness and wear resistance, while the final response depends on carburizing temperature, case structure, carbide population, and retained austenite [10-13]. These relationships suggest that thermochemical treatment can be used not only for bulk steels but also for appropriately designed electrodeposited iron-rich coatings.

The tribological performance of a restoration coating cannot be assessed from hardness alone. Comparative studies of hard-chromium replacements and electroless nickel-based coatings demonstrate that wear, scuffing, and coating integrity depend on the combined effect of microstructure, hard phases, contact conditions, and post-deposition treatment [7, 8, 14, 15]. Recent reviews and methodological studies of industrial chromium electrodeposition further show that Cr(III) baths can be engineered to produce comparatively thick, hard deposits while reducing the environmental burden associated with Cr(VI)-based processes [16-18]. Consequently, a repair

process intended for precision diesel components should be evaluated by linking deposition conditions with coating structure, hardness, seizure resistance, and wear in a fuel-lubricated contact. In particular, tribological investigations of chromium- and chromium-alloy coatings deposited from trivalent baths confirm that wear behavior is governed by coating structure and can change substantially after thermal treatment [19-21].

Despite the extensive literature on chromium electrodeposition, hard-chromium alternatives, and carburized steels, the combined use of electrodeposited iron–chromium coatings followed by carburizing has received limited attention for restoring precision diesel fuel-equipment components. In particular, the effect of chromium content on carburized-layer development and the relation between thermochemical-treatment temperature and tribological behavior require clarification.

The aim of this work was to determine how carburizing and subsequent quenching and tempering affect the structure, chromium-dependent hardening response, seizure resistance, and wear resistance of electrodeposited iron–chromium coatings, and to assess their applicability to restoration of precision fuel-equipment components.

2. MATERIALS AND METHODS

2.1 Electrodeposition and carburizing

Electrochemical iron–chromium coatings were deposited on normalized KhVG steel (a Russian chromium–tungsten–manganese alloy tool steel) specimens from a sulfate electrolyte based on ferrous sulfate $FeSO_4 \cdot 7H_2O$ and chromium nitrate $Cr(NO_3)_3 \cdot 9H_2O$. The carburizing mixture contained the following components (wt.%): 250–400 $FeSO_4 \cdot 7H_2O$, 5–20 $Cr(NO_3)_3 \cdot 9H_2O$, and 20–40 Na_2SO_4. The pH was maintained at 1.0–1.5. Deposition was performed at 20 °C using asymmetric alternating current at industrial frequency. The ratio of cathodic to anodic current components was $\beta = 6$; the cathodic current density D_k was 40–50 A/dm² for the principal coating regime.

To increase hardness and wear resistance, the iron–chromium coatings were carburized in a highly active paste based on amorphous carbon. The carburizing mixture contained the following components (wt.%): 60 DG-100 gas carbon black, 10 $BaCO_3$, and 30 polyvinyl acetate emulsion. A 5–6 mm layer of paste was applied to each specimen. After drying, the specimens were placed in sealed containers, and the remaining volume was filled with spent charcoal carburizer. The carburizing temperature was varied from 860 to 950 °C and the holding time from 1 to 10 h. The carburized specimens were then heated for quenching in a TP-2 furnace within 780–1000 °C, oil-quenched, and tempered at 150–600 °C; the specific regimes used for the hardness and tribological series are stated below.

2.2 Structural and compositional characterization

Coating structure and morphology were examined by optical microscopy and scanning electron microscopy (SEM). Metallographic observations were performed with an Olympus GX51 microscope, and SEM and energy-dispersive X-ray spectroscopy (EDS) were carried out using a Quanta 600 FEG microscope. Chromium content in the electrodeposited coatings was quantified by EDS on polished coating cross-sections and is reported in wt.% in Section 3.1. Rockwell C hardness (HRC) was measured with an AFFRI URBV-VRS tester using a 120° diamond cone, a 98.07 N preliminary test force, and a 1471 N total test force. The historical laboratory record available for this revision does not preserve the total-force dwell-time setting; therefore, no unverified dwell-time value has been introduced into the manuscript.

2.3 Tribological testing

Wear and seizure resistance were evaluated on an II-5018 friction machine using a disk–block configuration. The disks were made of KhVG steel and carried 0.5 mm iron–chromium coatings carburized under the specified conditions, oil-quenched from 880 °C, and tempered at 200 °C. Hardened ShKh15 steel (a high-carbon chromium bearing steel) blocks were used as counterbodies. For dry-friction seizure tests, contact pressure was increased by 0.25 MPa after every 2 min of operation; the test was stopped when seizure bands appeared on the disk together with a distinct increase in machine vibration. For diesel-fuel tests, fuel was supplied to the contact at 20 drops/min, nominal pressure was 5 MPa, and test duration was 2–6 h. Wear was determined gravimetrically using PA214C analytical balances with 0.0001 g readability. The weighing error was taken as no greater than ±0.0003 g per weighing and ±0.0006 g for the difference between two weighings. With the corrected wear unit used in the mass-loss results ($\times 10^{-3}$ g), the corresponding relative uncertainty ranges from approximately 1.6% to 7.5% over the reported mass-loss interval. The archived dataset contains one reported value for each hardness, seizure, and wear condition but does not preserve replicate-level measurements or the number of independent repeats for the historical tests. Accordingly, the results are presented as individual experimental values rather than means; SD values and error bars were not reconstructed retrospectively.

3. RESULTS AND DISCUSSION

3.1 Deposition kinetics and chromium content

Deposition rate is an important characteristic of iron–chromium coating formation because it determines both restoration productivity and the conditions under which the coating structure develops. The effect of cathodic current density was therefore investigated. Coatings were deposited from an electrolyte containing 350 kg/m³ $FeSO_4 \cdot 7H_2O$, 20 kg/m³ $Cr(NO_3)_3 \cdot 9H_2O$, and 20 kg/m³ Na_2SO_4 under asymmetric alternating current ($\beta = 6$), while the cathodic current density was varied from 10 to 60 A/dm². The results are shown in Figure 1.

The experimental deposition rate increased monotonically with cathodic current density over the investigated range, while the calculated curve reproduced the overall nonlinear trend (Figure 1). The increase became progressively smaller at higher D_k, indicating a transition toward a regime in which further current-density growth produced diminishing gains in coating growth rate. This representation is used only to describe the measured iron–chromium deposition data; Figure 1 does not compare the coating with pure iron.

The deposition rate also depended on the $FeSO_4 \cdot 7H_2O$

concentration. Increasing this concentration from 300 to 400 kg/m³ raised the coating growth rate from 0.23 to 0.30 mm/h, or by approximately 1.3 times. By contrast, varying $Cr(NO_3)_3 \cdot 9H_2O$ from 5 to 20 kg/m³ had no pronounced effect on deposition rate.

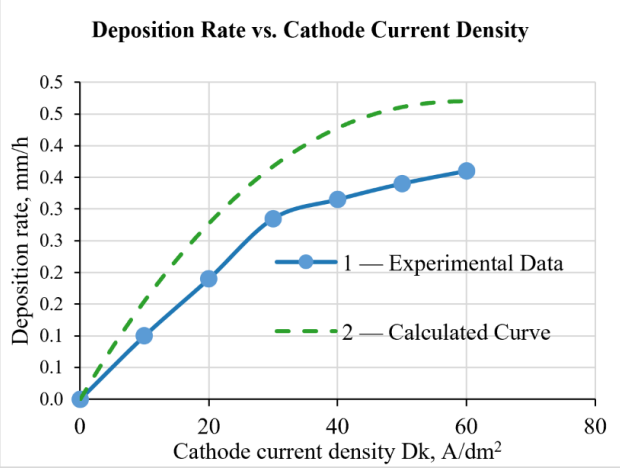


Figure 1. Effect of cathodic current density on iron–chromium coating deposition rate: 1–experimental data; 2–calculated approximation

Chromium content in the electrodeposited coating, determined by EDS, was governed primarily by chromium nitrate concentration (Figure 2). The measured chromium content increased from 2.1 wt.% at 5 kg/m³ $Cr(NO_3)_3 \cdot 9H_2O$ to approximately 7.8 wt.% at 20 kg/m³. A further increase in chromium salt concentration produced no meaningful increase in chromium incorporation and was accompanied by a lower deposition rate.

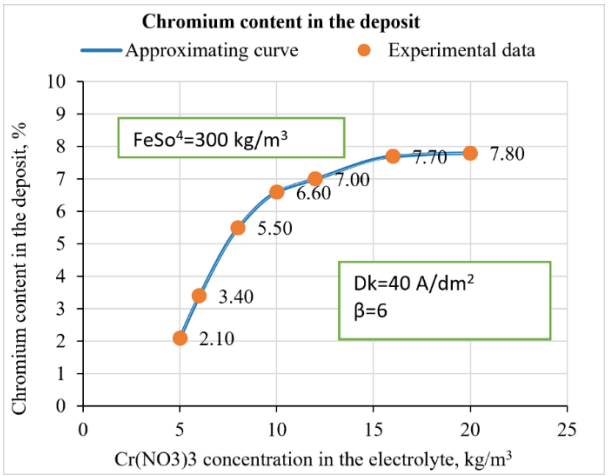


Figure 2. Energy-dispersive X-ray spectroscopy (EDS)-determined chromium content in the electrodeposited iron–chromium coating as a function of chromium nitrate concentration

This behavior is probably related to changes in the cathode-adjacent layer. Chromium nitrate supplies Cr^{3+} and NO_3^- ions, changes local deposition conditions, and indirectly affects chromium incorporation into the growing coating. This can explain why the limiting chromium content was reached at a relatively low chromium salt concentration. Increasing $Cr(NO_3)_3 \cdot 9H_2O$ beyond this level did not raise the chromium content and was accompanied by slower deposition.

A ferrous-sulfate electrolyte containing chromium nitrate therefore produces iron–chromium coatings with chromium levels comparable to those of several structural and tool steels. This creates the possibility of deliberately changing coating structure and properties through subsequent thermochemical treatment.

3.2 Microstructure and formation of the carburized layer

Microstructural analysis showed that the electrodeposited iron–chromium coatings produced under all investigated electrolysis conditions had a pronounced layered structure. The layering was clearly visible metallographically (Figure 3) and became more pronounced as cathodic current density increased. Cracks appeared at current densities above 50 A/dm², indicating greater structural heterogeneity and deterioration of mechanical properties.



Figure 3. Microstructure of an iron–chromium deposit produced by asymmetric alternating current (β = 6) at D_k = 40 A/dm²

Layered structures are characteristic not only of iron–chromium coatings but also of many other iron-based electrodeposits [5]. Their formation mechanism remains under discussion. According to one interpretation, layers form because metal ions are periodically depleted in the cathode-adjacent region. Another explanation relates the layers to local alkalization and periodic formation of iron hydroxides [6, 7]. Irrespective of the exact mechanism, pronounced layering is an unfavorable structural feature that can reduce coating performance.

Carburizing was applied to reduce structural heterogeneity and improve the physicomechanical properties of the electrodeposited iron–chromium coatings. Heating during carburizing activates diffusion, weakens the layered pattern, redistributes alloying and interstitial elements, and forms a hardened surface zone. Carbon enrichment simultaneously changes the coating composition and properties toward those of the high-carbon steels used for the restored components.

Carburizing in the carbonate–carbon-black paste produced diffusion layers enriched with carbides. The carbide content and distribution depended on the chromium concentration in the coating (Figure 4).

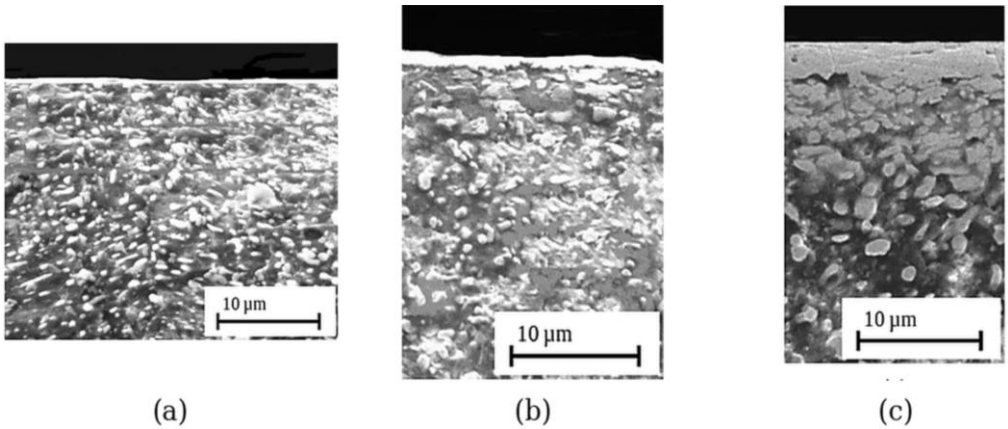


Figure 4. Microstructures (×500) of carburized iron–chromium coatings containing (a) 0.95% Cr, (b) 1.51% Cr, and (c) 3.07% Cr

Metallographic examination showed that the amount and distribution of carbide-rich constituents and the apparent diffusion-layer depth depended on chromium content. The most developed carburized layer was observed at approximately 1.5–2.0 wt.% Cr. At lower chromium content, the carbide-rich constituent was less pronounced, whereas at 3.07 wt.% Cr, the carburized-layer depth was reduced (Figure 4). The available microstructural and hardness data are summarized in Table 1.

Raising the carburizing temperature to 950 °C intensified carbon penetration and increased diffusion depth. For an electrodeposited coating containing approximately 2 wt.% Cr, the carburizing rate was 0.15–0.18 mm/h at 900 °C and 0.20–0.22 mm/h at 950 °C. For the 0.15–0.20 mm coating thickness typical of restored precision components, a 2–3 h treatment provided nearly through-thickness carbon enrichment. Model specimens with 0.5 mm coatings were used in laboratory tribological tests to ensure reproducible specimen preparation and testing.

Table 1. Summary of the effect of chromium content on carburized-layer development and hardness

Chromium Content, wt.%	Carburized-Layer Response and Hardness
0.95	Lower carbide-rich fraction and less-developed layer; maximum HRC = 66.5
1.48–1.51	Most developed layer and greatest carbide-rich fraction; maximum HRC = 69.5
3.07	Reduced carburizing depth at higher Cr content; HRC not determined

3.3 Hardness after quenching and tempering

The final hardness response was established by quenching and tempering. Coatings containing 0.95 and 1.48–1.50 wt.% Cr were carburized at 900 °C for 3 h. The quenching temperature was varied from 800 to 900 °C for the hardness series shown in Figures 5 and 6, followed by tempering at 200 or 300 °C. The curves report HRC values obtained under the Rockwell C conditions specified in Section 2.2.

The coating containing 1.48 wt.% Cr exhibited higher hardness than the coating containing 0.95 wt.% Cr because its diffusion layer contained a larger fraction of high-hardness carbides.

Regardless of chromium content, maximum hardness was obtained after quenching from 840–860 °C. This behavior is attributed to martensite formation in the regions between carbide particles. At higher quenching temperatures, carbides partially dissolved and the solid solution became excessively enriched with carbon. Rapid cooling then produced a substantial amount of retained austenite together with martensite. Because retained austenite is softer, the integral coating hardness decreased.

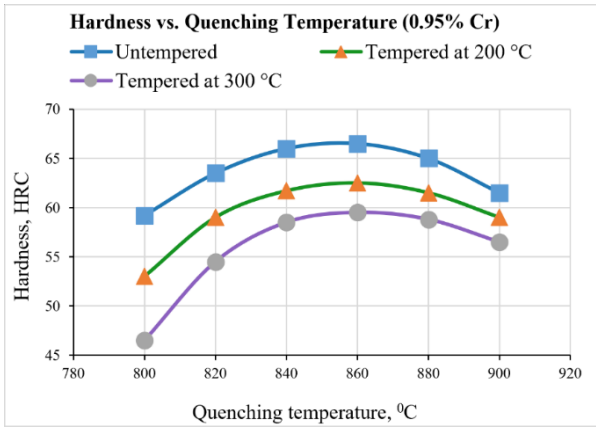


Figure 5. Effect of quenching temperature on the hardness of a carburized iron–chromium coating containing 0.95% Cr: 1–untempered; 2–tempered at 200 °C; 3–tempered at 300 °C

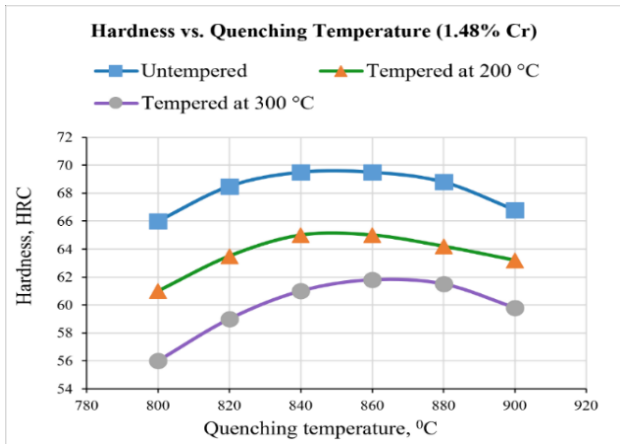


Figure 6. Effect of quenching temperature on the hardness of a carburized iron–chromium coating containing 1.48% Cr: 1–untempered; 2–tempered at 200 °C; 3–tempered at 300 °C

Tempering temperature also had a strong effect. Increasing the tempering temperature reduced hardness almost

independently of chromium content. Tempering at 200 °C decreased hardness by approximately 5 HRC, while tempering at 300 °C decreased it by approximately 10 HRC. These changes can be related to structural transformations in the diffusion layer and substrate.

The hardness trends are consistent with the development of hard carbide-rich constituents during carburizing. Their amount, distribution, and the response of the surrounding matrix to quenching jointly determine the integral HRC value and are also expected to influence seizure and wear behavior.

3.4 Seizure and wear resistance

The effect of carburizing on tribological behavior was evaluated using KhVG steel specimens with iron–chromium coatings carburized at different temperatures and holding times, thereby producing different hardened-layer conditions. All specimens in the seizure and diesel-fuel wear series were oil-quenched from 880 °C and tempered at 200 °C. Testing was performed under dry friction and in diesel fuel to represent two limiting contact conditions relevant to fuel-pump plunger pairs.

Under dry friction, the load at which seizure occurred was determined using a carburized iron–chromium-coated disk against hardened ShKh15 steel blocks on the II-5018 machine. The pressure was increased by 0.25 MPa after every 2 min of operation and testing was stopped at the onset of visible seizure bands and pronounced machine vibration. The resulting critical seizure pressure is shown in Figure 7.

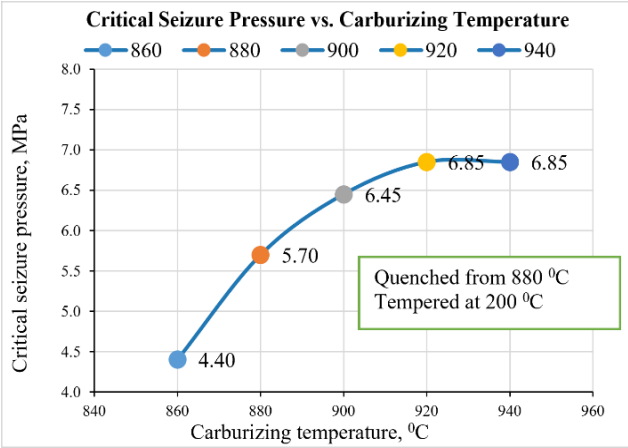


Figure 7. Critical seizure pressure under dry friction as a function of carburizing temperature

Increasing the carburizing temperature improved seizure resistance, with the maximum values reached at 920–940 °C. This trend coincided with the more strongly developed carbide-rich surface structure observed after higher-temperature carburizing, which increased resistance to adhesive contact damage under dry friction.

Because fuel-equipment components operate in contact with diesel fuel, additional tests were conducted with fuel supplied to the friction zone under the conditions specified in Section 2.3. Coated disks carburized at 860–940 °C were oil-quenched from 880 °C and tempered at 200 °C. The mass-loss results are summarized in Table 2.

Mass loss in diesel fuel decreased as carburizing temperature increased to 920–940 °C, and the difference became most evident at the 6 h test duration. After 6 h, the coating carburized at 920 °C showed a mass loss of 12 × 10^{-3} g compared with 37 × 10^{-3} g after carburizing at 860 °C, i.e., approximately a 3.1-fold reduction under the same test duration and contact conditions.

The lower mass loss after carburizing at 920–940 °C is consistent with the more developed hardened surface layer, which increases resistance to microcutting, microplastic deformation, and adhesive interaction with the counterbody. The present tests establish a comparative laboratory trend; they do not by themselves constitute a service-life comparison with new plunger pairs.

Table 2. Mass loss of carburized iron–chromium coatings containing 1.48 wt.% Cr at different carburizing temperatures

Test Time, h	Carburizing Temperature, °C				
	860	880	900	920	940
2	14	12	10	8	10
4	23	18	11	9	9
6	37	32	28	12	13

Note: Mass loss is expressed as ×10^{-3} g; absolute uncertainty from two weighings was taken as ±0.0006 g, corresponding to approximately 1.6–7.5% of the reported values.

Taken together, the deposition, microstructural, hardness, seizure, and fuel-lubricated wear results show that carburizing is an effective means of changing the functional response of electrodeposited iron–chromium coatings. The data support selecting the chromium content and thermochemical-treatment regime jointly rather than treating them as independent parameters.

4. CONCLUSIONS

Electrodeposited iron–chromium coatings produced under asymmetric alternating current had a pronounced layered structure in the as-deposited condition. Carburizing reduced the visual prominence of this layering and formed a carbon-enriched, carbide-containing surface diffusion layer whose development depended on chromium content and treatment temperature.

The most favorable combination in the investigated chromium range was obtained at approximately 1.5–2.0 wt.% Cr: the 1.48–1.51 wt.% Cr coating showed the greatest apparent carburized-layer development and reached about 69.5 HRC in the quenching series. Maximum hardness occurred after quenching from 840–860 °C. In tribological tests, carburizing at 920–940 °C produced the highest critical seizure pressure and the lowest mass loss in diesel fuel.

The results support carburized iron–chromium electrodeposits as a technically promising restoration coating for precision diesel fuel-equipment components. However, the present laboratory tests address structure, hardness, seizure resistance, and short-duration wear only. A claim of service life comparable with new plunger pairs requires separate long-term bench or field endurance tests under matched operating conditions.

REFERENCES

[1] Laoucine, Stępień, Z. (2019). The influence of particulate contamination in diesel fuel on the damage to fuel injection systems. Combustion Engines, 177(2): 76-82. https://doi.org/10.19206/CE-2019-213

[2] Bejger, A., Drzewieniecki, J.B. (2020). A new method of identifying the limit condition of injection pump wear in self-ignition engines. Energies, 13(7): 1601. https://doi.org/10.3390/en13071601
[3] Qu, J., Truhan, J.J., Blau, P.J. (2005). Investigation of the scuffing characteristics of candidate materials for heavy duty diesel fuel injectors. Tribology International, 38(4): 381-390. https://doi.org/10.1016/j.triboint.2004.08.018
[4] Giovanardi, R., Orlando, G. (2011). Chromium electrodeposition from Cr(III) aqueous solutions. Surface and Coatings Technology, 205(15): 3947-3955. https://doi.org/10.1016/j.surfcoat.2011.02.027
[5] Okonkwo, B.O., Jeong, C., Lee, H.B., Jang, C., Rahimi, E., Davoodi, A. (2023). Development and optimization of trivalent chromium electrodeposit on 304L stainless steel to improve corrosion resistance in chloride-containing environment. Heliyon, 9(12): e22538. https://doi.org/10.1016/j.heliyon.2023.e22538
[6] Sheu, H.H., Lin, M.H., Jian, S.Y., Hong, T.Y., Hou, K.H., Ger, M.D. (2018). Improve the mechanical properties and wear resistance of Cr-C thin films by adding Al_2O_3 particles. Surface and Coatings Technology, 350: 1036-1044. https://doi.org/10.1016/j.surfcoat.2018.02.069
[7] Wasekar, N.P., Sundararajan, G. (2015). Sliding wear behavior of electrodeposited Ni-W alloy and hard chrome coatings. Wear, 342-343: 340-348. https://doi.org/10.1016/j.wear.2015.10.003
[8] Allahyarzadeh, M.H., Aliofkhazraei, M., Rezvanian, A.R., Torabinejad, V., Sabour Rouhaghdam, A.R. (2016). Ni-W electrodeposited coatings: Characterization, properties and applications. Surface and Coatings Technology, 307: 978-1010. https://doi.org/10.1016/j.surfcoat.2016.09.052
[9] Saeki, R., Yakita, T., Ohgai, T. (2022). Magnetization and microhardness of iron-chromium alloy films electrodeposited from an aqueous solution containing N,N-dimethylformamide. Journal of Materials Research and Technology, 18: 2735-2744. https://doi.org/10.1016/j.jmrt.2022.03.183
[10] Tarakci, M., Korkmaz, K., Gencer, Y., Usta, M. (2005). Plasma electrolytic surface carburizing and hardening of pure iron. Surface and Coatings Technology, 199(2-3): 205-212. https://doi.org/10.1016/j.surfcoat.2005.02.117
[11] de Souza Lamim, T., Anselmo, L.M., Bendo, T., et al. (2022). Effect of low-temperature plasma carburizing on surface topography, mechanical and tribological properties of sintered iron and nitrided sintered iron. Tribology International, 168: 107452. https://doi.org/10.1016/j.triboint.2022.107452
[12] Li, B., Li, C., Wang, Y., Jin, X. (2018). Effect of cryogenic treatment on microstructure and wear resistance of carburized 20CrNi2MoV steel. Metals, 8(10): 808. https://doi.org/10.3390/met8100808
[13] Ionescu, L., Pantawane, M., Tănase, C., Sichim, R., Dascălu, C., Ghiban, B. (2023). Evaluation of retained austenite in carburized bearing steel using magneto-inductive method. Crystals, 13(8): 1173. https://doi.org/10.3390/cryst13081173
[14] Mukhopadhyay, A., Barman, T.K., Sahoo, P., Davim, J.P. (2018). Comparative study of tribological behavior of electroless Ni-B, Ni-B-Mo, and Ni-B-W coatings at room and high temperatures. Lubricants, 6(3): 67. https://doi.org/10.3390/lubricants6030067
[15] Georgiou, E.P., Drees, D., Timmermans, G., et al. (2021). High performance accelerated tests to evaluate hard Cr replacements for hydraulic cylinders. Coatings, 11(12): 1511. https://doi.org/10.3390/coatings11121511
[16] Okonkwo, B.O., Jeong, C., Jang, C. (2022). Advances on Cr and Ni electrodeposition for industrial applications—A review. Coatings, 12(10): 1555. https://doi.org/10.3390/coatings12101555
[17] Xu, L., Pi, L., Dou, Y., et al. (2020). Electroplating of thick hard chromium coating from a trivalent chromium bath containing a ternary complexing agent: A methodological and mechanistic study. ACS Sustainable Chemistry & Engineering, 8(41): 15540-15549. https://doi.org/10.1021/acssuschemeng.0c04529
[18] Protsenko, V. (2025). A review on electrodeposition and tribological performance of chromium-based coatings from eco-friendly trivalent chromium baths. Discover Electrochemistry, 2: 22. https://doi.org/10.1007/s44373-025-00037-7
[19] Bikulčius, G., Češunienė, A., Selskienė, A., Pakštas, V., Matijošius, T. (2017). Dry sliding tribological behavior of Cr coatings electrodeposited in trivalent chromium sulphate baths. Surface and Coatings Technology, 315: 130-138. https://doi.org/10.1016/j.surfcoat.2017.01.076
[20] Zeng, Z., Wang, L., Liang, A., Zhang, J. (2006). Tribological and electrochemical behavior of thick Cr-C alloy coatings electrodeposited in trivalent chromium bath as an alternative to conventional Cr coatings. Electrochimica Acta, 52(3): 1366-1373. https://doi.org/10.1016/j.electacta.2006.07.038
[21] Mardanifar, A., Mohseni, A., Mahdavi, S. (2021). Wear and corrosion of Co-Cr coatings electrodeposited from a trivalent chromium solution: Effect of heat treatment temperature. Surface and Coatings Technology, 422: 127535. https://doi.org/10.1016/j.surfcoat.2021.127535

NOMENCLATURE

β	ratio of cathodic to anodic current components (dimensionless)
D_k	cathodic current density, A/dm²
HRC	Rockwell hardness, C scale (dimensionless)
pH	hydrogen-ion activity index (dimensionless)